HHS Public Access

Author manuscript

Respir Physiol Neurobiol. Author manuscript; available in PMC 2023 January 01.

Published in final edited form as:

Respir Physiol Neurobiol. 2022 January ; 295: 103780. doi:10.1016/j.resp.2021.103780.

Mitochondrial Morphology and Function Varies Across Diaphragm Muscle Fiber Types

Alyssa D. Brown, **Matthew J. Fogarty**, **Gary C. Sieck**[#]

Department of Physiology & Biomedical, Mayo Clinic, Rochester, MN 55905

Abstract

In diaphragm muscle (DIAm), type I and IIa fibers are recruited to accomplish breathing, while type IIx/IIb fibers are recruited only during expulsive/straining behaviors. Thus, type I and IIa DIAm fibers are much more active (duty cycle of ~40%) than type IIx/IIb fibers (duty cycle of <1%), which we hypothesized underlies intrinsic differences in mitochondrial structure and function. MitoTracker Green labeled mitochondria were imaged in 3-D using confocal microscopy. Mitochondrial volume density (MVD, per muscle fiber volume) was higher, and mitochondria were more filamentous in type I and IIa DIAm compared to type IIx/IIb fibers. The maximum velocity of the succinate dehydrogenase reaction (SDH_{max}), measured using a quantitative histochemical technique was found to be higher in type I and IIa DIAm fibers compared to type IIx/IIb fibers with and without normalizing for MVD. These results are consistent with fiber type differences in the intrinsic structural and functional properties of DIAm fibers and closely match differences in energetic demands.

Keywords

diaphragm; mitochondria; mitochondrial function; confocal microscopy; succinate dehydrogenase

1. INTRODUCTION

The diaphragm muscle (DIAm) in mammals is the primary muscle involved in inspiration, although it also contributes to higher force airway protective and straining behaviors. Neural control of the DIAm during inspiration involves recruitment of fatigue resistant slow and fast motor units comprising type I and IIa fibers (Sieck & Fournier, 1989; Sieck, 1991; Sieck *et al.*, 1996; Fogarty & Sieck, 2019). In contrast, higher force airway protective and

[#]Correspondence: Gary C. Sieck, PhD, Vernon F. and Earline D. Dale Professor, Distinguished Mayo Investigator, Department of Physiology & Biomedical Engineering, Mayo Clinic, 200 1st St SW, Rochester, MN 55905, Phone: (507) 284 6850, sieck.gary@mayo.edu.

CRediT Author Statement

Alyssa D. Brown: Conceptualization, Methodology, Formal Analysis, Investigation, Writing-Original Draft

Matthew J. Fogarty: Conceptualization, Methodology, Formal Analysis, Investigation, Writing-Review & Editing

Gary C. Sieck: Conceptualization, Methodology, Formal Analysis, Investigation, Writing-Review & Editing

Disclosure of Conflicts of Interest: None of the authors has any conflicts of interest, real nor perceived, to disclose.

expulsive/straining behaviors of the DIAm, require recruitment of more fatigable fast motor units comprising type IIx/IIb fibers (Sieck & Fournier, 1989; Sieck, 1991; Sieck *et al.*, 1996; Fogarty & Sieck, 2019). Because of their recruitment during breathing, type I and IIa fibers are much more active with a duty cycle of ~40%, whereas type IIx/IIb fibers are infrequently activated with a duty cycle of <1% (Sieck & Fournier, 1989; Sieck, 1991; Fogarty & Sieck, 2019). The varying levels of activity have markedly different energetic requirements for mitochondrial support.

Previously, we used 2-D electron microscopy (EM) to estimate mitochondrial volume densities in type identified DIAm fibers and found that type I and IIa DIAm fibers have higher mitochondrial volume densities than type IIx/IIb fibers (Sieck *et al.*, 1998). These estimates of mitochondrial volume densities were based on a very small sample of type-identified fibers per DIAm due to the limitations of EM. In the present study, we developed a technique to label mitochondria in DIAm fibers using MitoTracker, followed by 3-D imaging and reconstruction using confocal microscopy. Using this technique, we were able to evaluate mitochondrial volume density and morphology in a much larger sample of type identified DIAm fibers. Furthermore, in the same DIAm fibers we were able to determine mitochondrial function by measuring the maximum velocity of the succinate dehydrogenase reaction (SDH_{max}) using a quantitative histochemical technique (Sieck *et al.*, 1986; Blanco *et al.*, 1988). In previous studies using this technique, we found that type I and IIa DIAm fibers have higher SDH_{max} than IIx/IIb fibers (Sieck *et al.*, 1986; Enad *et al.*, 1989; Sieck *et al.*, 1989; Sieck *et al.*, 1995; Sieck *et al.*, 1996; Lattari *et al.*, 1997; Fogarty *et al.*, 2020). However, in these previous studies, we did not assess whether fiber type differences in SDH_{max} were associated with mitochondrial volume density or morphology.

In skeletal muscles in mice, mitochondria in type I and IIa fibers are more filamentous compared to type IIx/IIb fibers (Mishra *et al.*, 2015). In primary human skeletal muscle cells (hSkMCs), we found that mitochondrial fusion induced by vitamin D ($1\alpha,25(OH)_2D_3$) is associated with increased O_2 consumption rate determined by respirometry (Ryan *et al.*, 2016). Recently, in human airway smooth muscle cells exposed to tumor necrosis factor α (TnFα), we found that mitochondrial fragmentation is associated with reduced maximum O_2 consumption rate even when normalized for changes in mitochondrial volume (Delmotte *et al.*, 2017; Delmotte & Sieck, 2019). These results suggest there are intrinsic differences in mitochondrial function that depend on mitochondrial morphology. The purpose of the present study was to determine mitochondrial volume, mitochondrial morphology, and SDH_{max} in the same type identified DIAm fibers. We hypothesized that in type I and IIa DIAm fibers: 1) mitochondrial volume densities are higher, 2) mitochondrial morphology is more filamentous, and 3) intrinsic SDH_{max} (normalized for mitochondrial volume) is higher as compared to type IIx/IIb fibers, due to increased fusion of mitochondrial networks.

2. MATERIALS AND METHODS

2.1 Ethical approval

All procedures were performed in accordance with the American Physiological Society's Animal Care Guidelines, the National Institutes of Health (NIH) guide for the use and care

of laboratory animals (NIH Publications #8023, revised 1978) and were approved by the Institutional Animal Care and Use Committee (IACUC) at Mayo Clinic.

2.2 Experimental animals

In the present study, 6 pathogen-free Sprague-Dawley rats (300–370 g) (3 males and 3 females) were obtained from Envigo (Indianapolis, IN) and allowed at least 1 week to acclimate before experiments. Animals were maintained two animals of the same sex per cage under an alternating 12:12 h light-dark cycle with *ad libitum* access to rat chow and fresh water.

2.3 Tissue collection and processing

Rats were deeply anesthetized with intraperitoneal injection of ketamine (80 mg/kg) and xylazine (20 mg/kg) and then euthanized by exsanguination. The DIAm was excised and placed in a tray of Rees-Simpson solution (containing, in mM: 135 Na^+, 5 K^+, 2 Ca^{2+}, 1 Mg^{2+}, 120 Cl^-, and 25 HCO_3^-) bubbled with carbogen gas (95% O_2-5% CO_2) at room temperature. While in solution, an ~2 mm wide DIAm strip was dissected from the right mid-costal region. As previously described the DIAm strip was stretched to 150% of resting length to approximate L_0 and fresh-frozen on cork in melting isopentane cooled by liquid nitrogen (Prakash *et al.*, 1993a; Zhan *et al.*, 1997). All measurements were made in the same DIAm fibers identified in alternate serial transverse sections cut at different thicknesses (depending on the measurement) using a cryostat (Reichert Jung Frigocut 2800 Cryostat, Reichert Microscope Services, Depew, NY, USA) kept at −30°C.

2.4 Muscle fiber type classification

Muscle fiber type classification was based on immunoreactivity for different MyHC isoforms as previously described in detail (Sieck *et al.*, 1996; Fogarty *et al.*, 2019). Briefly, 10 μm sections were fixed in 4% paraformaldehyde for 10 min before being incubated overnight at 4°C in solutions containing primary antibodies for $MyHC_{Slow}$ (NBP2 (IgG), 1:25 dilution; Novus), $MyHC_{2A}$ (N1551 (IgM), 1:1 dilution; Novus), and $MyHC_{2X}$ (NBP1 (IgG), 1:10 dilution; Novus). To determine fiber type based on immunoreactivity for MyHC isoforms, three alternate serial sections were used with different fluorescently conjugated secondary antibodies. To visualize immunoreactivity for $MyHC_{Slow}$ and $MyHC_{2A}$ isoforms in the same section, IgG-Alexa-594 and IgM-Cy5 secondary antibody conjugated secondary antibodies were applied, respectively at a 1:200 dilution (Figure 1). In a second alternate section of the same fibers, immunoreactivity for the $MyHC_{2X}$ isoform was visualized using a IgG-Alexa-594 conjugated secondary antibody (1:200 dilution). Based on the pattern of immunoreactivity, DIAm fibers were classified as type I (immunoreactivity for $MyHC_{Slow}$), type IIa (immunoreactivity for $MyHC_{2A}$), and type IIx/IIb (immunoreactivity for $MyHC_{2X}$). In previous studies on single dissected DIAm fibers, we found that most fibers expressed a single MyHC isoform (i.e., $MyHC_{Slow}$ and $MyHC_{2A}$). However, many of the DIAm fibers expressing the $MyHC_{2X}$ isoform also expressed the $MyHC_{2B}$ isoform in varying proportions (Geiger *et al.*, 1999; Geiger *et al.*, 2000; Han *et al.*, 2003; Geiger *et al.*, 2006). Unfortunately, we were unable to validate the antibody for $MyHC_{2B}$ in DIAm fibers. Accordingly, DIAm fibers that were immunoreactive for $MyHC_{2X}$ were classified as type IIx/IIb. Fluorescence immunoreactivity in DIAm fibers was imaged using a 40x oil-immersion objective (NA

1.4) on an Olympus FV2000 laser confocal microscope capable of sequential multi-color fluorescence imaging. Images were captured at 16-bit resolution (1,096 gray levels) in a 1,024 × 1,024 pixel array, with similar acquisition parameters across preparations.

2.5 Mitochondrial labeling and imaging

In 10 μm thick serial sections of the same DIAm fibers, mitochondria were labeled using MitoTracker Green. In this procedure, sections were placed in a solution containing 1.5 μL MitoTracker Green in 5 mL PBS for 30 min. The sections were then washed three times with PBS for 10 min each wash and cover-slipped for imaging. Labeled mitochondria within DIAm fibers were visualized using an Olympus FV2000 laser scanning confocal microscope (Olympus Life Sciences Solutions, Waltham, MA) equipped with argon (488 nm) and green HeNe (543 nm) lasers. The 3-D confocal imaging techniques used have been previously reported in detail (Prakash *et al.*, 1993b, 1994; Sieck *et al.*, 1999; Delmotte *et al.*, 2017). Briefly, all images were acquired at 16-bit resolution (1,096 gray levels) in a 1024×1024 pixel array using a 40× Plan Apo oil-immersion objective (NA 1.40). The empirically calculated point spread function for the 40× objective was used to set a Z-axis step size of 0.5 μm, as previously reported (Prakash *et al.*, 1993b, 1994; Sieck *et al.*, 1999; Fogarty *et al.*, 2018). Based on calibration, the voxel dimensions were 0.207 μm X-axis, 0.207 μm Y-axis, and 0.5 μm Z-axis resulting in 0.021 μm^3 voxels. Laser intensity and photomultiplier settings were adjusted to maintain black level of the blank sections. This was accomplished by defining a region of interest (ROI) in a portion of the image with no MitoTracker Green signal. This black level was adjusted such the gray levels were not saturated but also <10% of the dynamic range. Another ROI was delineated in an area displaying the most intense MitoTracker Green fluorescence and the gain was adjusted to maximize the dynamic range while preventing saturation. To improve spatial resolution of the images, a blind deconvolution algorithm (Point Scan Confocal, 3 iterations; NIS-Elements; Nikon Instruments Inc., RRID:SCR_014329) was applied for each 2-D image in the Z-stack as previously described (Fogarty *et al.*, 2021). This algorithm estimates the idealized point spread function for a given image, thus obviating the need to obtain a point spread function for the optical system for each image acquisition session. The deconvolution algorithm increases the spatial resolution approximately two-fold to ~125 nm (Fogarty *et al.*, 2021). The deconvolved images were then further processed for background correction, ridge filter detection, skeletonization, and thresholding with ImageJ (imagej.nih.gov/ij/, Fiji, RRID:SCR_002285), as previously described (Donoho & Johnstone, 1994; Koopman *et al.*, 2005a; Koopman *et al.*, 2005b; Koopman *et al.*, 2006; Delmotte *et al.*, 2017; Chaudhry *et al.*, 2020; Fogarty *et al.*, 2021). MitoTracker Green fluorescence gray levels in the images were thresholded to identify voxels containing MitoTracker Green fluorescence using the Default method in ImageJ/Fiji software and binary images created (Aravamudan *et al.*, 2014; Delmotte *et al.*, 2017; Chaudhry *et al.*, 2020). The deconvolved, processed and binarized images were then reconstructed in 3-D using ImageJ and NIS-Elements.

After 3-D reconstruction of binarized images in the Z-stack, the number of voxels within a delineated muscle fiber boundary was used to determine fiber volume. Similarly, the number of binarized voxels containing MitoTracker Green labeled mitochondria within each muscle fiber was used to determine mitochondrial volume (Figure 2). Mitochondrial volume density

was calculated as the ratio of mitochondrial volume to the total muscle fiber volume (fiber cross-sectional area × 10 μm section thickness). These measurements were performed using ImageJ/Fiji Mitochondria Analyzer plug-in.

Mitochondrial morphology was assessed using the same ImageJ/Fiji Mitochondria Analyzer plug-in. Two morphological measurements were determined: mean branch length (μm) and mitochondrial complexity index (MCI) (Vincent *et al.*, 2019). Additional measures included the total number of mitochondrial branches, total mitochondrial surface area and volume. MCI was calculated using the following equation:

$$MCI = \frac{SA^3}{16\pi^2 V^2}$$

Where SA is total mitochondrial surface area within a muscle fiber and V is the total mitochondrial volume within the muscle fiber.

2.6 Quantitative histochemical procedure for measuring SDH_{max}

The quantitative histochemical procedure for measuring the maximum velocity of the SDH reaction in single muscle fibers has been previously described in detail (Sieck *et al.*, 1986; Blanco & Sieck, 1987; Blanco *et al.*, 1988; Enad *et al.*, 1989; Watchko & Sieck, 1993; Proctor *et al.*, 1995; Sieck *et al.*, 1995; Sieck *et al.*, 1996; Zhan *et al.*, 1997). Briefly, alternate serial sections of DIAm fibers (the same fibers used for fiber type classification) were cut at 6 μm thickness and incubated in a solution containing 80 mM succinate, 1.5 mM nitro blue tetrazolium (NBT – reaction indicator), 5 mM EDTA, 0.2 mM mPMS, and 0.1 mM azide in 0.1 M phosphate buffer (pH=7.6). In previous studies, we determined that with succinate concentrations >80 mM the enzymatic reaction for SDH in muscle fibers was not substrate limited (Sieck *et al.*, 1986; Blanco *et al.*, 1988). In a separate series of experiments, the dependency of the SDH reaction on succinate concentration was re-assessed, and concentrations >80 mM were found to produce the maximum velocity of the SDH reaction in DIAm fibers. In the quantitative histochemical procedure, the progressive precipitation of a diformazan with the reduction of NBT (NBT_{dfz}) is used as the reaction indicator (Sieck *et al.*, 1986; Blanco *et al.*, 1988). Precipitation of NBT_{dfz} was quantified using an inverted light microscope (Olympus IX71, Olympus America, Melville, NY) with a 60× objective (1.0 NA). To calibrate for densitometry, an interference filter (570 nm) was used to limit the spectral range of the light source to the maximum absorption wavelength of NBT_{dfz}. Optical density (OD) was calibrated by imaging a series of known gray levels at 16-bit resolution (1,096 gray levels). The dynamic range during image acquisition was adjusted to take advantage of the full dynamic range while avoiding saturation of the images. A 200 μL solution without succinate was added to the cover slip, and a baseline image was acquired before adding a solution containing 80 mM succinate. Thereafter, images were repeatedly acquired every 15 s in a 1024 × 1024 pixel array using a digital camera (Hamamatsu ORCA Flash 4.0, Model C11440) (Figure 3A). The images were then processed using Metamorph software (Molecular Devices LLC., Sunnyvale, CA). The linearity of the SDH reaction was confirmed by measuring the change in OD in delineated muscle fibers every

15 s across a 10 min period (Figure 3B; r^2>0.99). The SDH_{max} was calculated using the Beer-Lambert-Bouguer law:

$$d[NBT_{dfz}]([fumarate])/dt = \frac{dOD/dt}{kl}$$

Where *OD* is the average OD within a region of interest (in this case the boundary of a DIAm fiber), *k* is the molar extinction coefficient of NBT_{dfz} (26,478 mol/cm) and *l* is the path length of light absorbance (6 μm). The SDH_{max} within the volume of individual DIAm fibers (fiber cross-sectional area × 6 μm section thickness) was expressed as mmol fumarate/L fiber/min. The dependency of OD measurements ([NBT_{dfz}] on path length was confirmed in a separate set of experiments (n=15 fibers per type) in which section thickness was varied from 4 to 10 μm. The relationship between OD and section thicknesses was linear for all fiber types.

In respirometry, basal and maximum respiratory capacity (O_2 consumption rate) are determined using a stress test that inhibits different complexes in the ETC and uncouples O_2 consumption from the proton (H^+) gradient (Ly & Ryall, 2017; Jacques *et al.*, 2020). To confirm that SDH_{max} reflected the maximum respiratory capacity of DIAm fibers, a similar stress test was used. The SDH reaction (with and without 80 mM succinate across a 10 min period) was assessed in three alternate serial sections (6 μm each) of DIAm fibers that were: untreated, treated with FCCP (1 mM to disrupt the proton gradient), and treated with rotenone (1 mM) to inhibit complex I of the ETC) and antimycin A (1 mM to inhibit complex III of the ETC) (Figure 3C). In each DIAm fiber type, treatment with FCCP, had no effect on SDH_{max} (Figure 3C). In contrast, treatment with a combination of rotenone and antimycin A, markedly slowed SDH_{max} across all DIAm fiber types (p<0.002 for all combinations, Bonferroni *post hoc* tests; n=15 fibers per type per animal; Figure 3C).

2.7 Statistical analysis

To ensure unbiased sampling of DIAm fibers, we used a stereological method in which image fields were initially selected at lower magnification (20X objective) to represent the entire thickness of the DIAm starting at the thoracic surface (top left corner of the image field) and moving in a diagonal direction toward the abdominal surface. Within the selected higher magnification image field, only DIAm fibers whose borders were contained within the image were sampled starting in the top left corner and moving in a diagonal direction to the lower right corner. Using this sampling method, approximately 8 fibers per higher magnification image field were sampled. Sampling continued until a total of 15 DIAm fibers per fiber type were included for each analysis. Previously, we found that 15 DIAm fibers per fiber type per animal is sufficient to detect differences in SDH_{max} of >25 % across fiber types (α=0.05, β=0.8) (Sieck *et al.*, 1996; Lattari *et al.*, 1997; Zhan *et al.*, 1997; Fogarty *et al.*, 2020). Although sex as a biological variable cannot be excluded, we previously observed no sex difference in the SDH_{max} of DIAm fibers (Fogarty *et al.*, 2020). However, sex was included as a biological variable in the statistical design and analysis. No sex differences were also observed in the present study, so data from both sexes were collapsed into single groups in the presentation of results. Data points that were greater than twice the standard

deviation from the mean were considered outliers and were excluded from analysis of this data.

We used Prism 8 for all data analyses (Graphpad, Carlsbad, CA). Each data set was assessed for normality with D'Agostino and Pearson tests. For comparisons between two groups, unpaired two-tailed Student's *t*-tests were used. For comparisons between three groups, one-way ANOVA, with Tukey's *post hoc* tests were performed. In cases where there were groups and factors, two-way ANOVA with Bonferroni *post hoc* tests were used. For comparisons of distributions, Kolmogorov-Smirnov tests were used. In order to determine if relationships between SDH_{max} and mitochondrial parameters were multi-modally distributed (i.e., were clustered in two or more groups), a runs test was performed. All data are reported as the mean ± 95% confidence interval of the mean, unless otherwise specified. Statistical significance was established at the $p<0.05$ level.

3. RESULTS

3.1 DIAm fiber type classification

Classification of type I and IIa DIAm fibers in the rat was unambiguous with clear immunoreactivity for the anti-$MyHC_{Slow}$ and anti-$MyHC_{2A}$ antibodies, respectively (Figure 1A). However, a clear distinction between type IIx and IIb DIAm fibers was not possible based on immunoreactivity for the anti-$MyHC_{2X}$ and anti-$MyHC_{All\text{-}but\text{-}2X}$ antibodies. We were unable to validate an anti-$MyHC_{2B}$ antibody for use in rat DIAm fibers. Some DIAm fibers that displayed immunoreactivity for the anti-$MyHC_{2X}$ antibody also showed immunoreactivity for the anti-$MyHC_{All\text{-}but\text{-}2X}$ antibody. These DIAm fibers likely co-express the $MyHC_{2B}$ isoform with $MyHC_{2X}$ isoform, consistent with previous studies examining MyHC isoform expression in single dissected DIAm fibers in the rat, where we showed that $MyHC_{2X}$ was singularly expressed in some fibers but typically co-expressed with $MyHC_{2B}$ in varying proportions (Geiger *et al.*, 1999; Geiger *et al.*, 2000; Han *et al.*, 2003; Geiger *et al.*, 2006). Within the DIAm, ~36 ± 2% were classified as type I, ~31 ± 3% as type IIa, and ~33 ± 5% as type IIx and/or IIb.

3.2 DIAm fiber cross-sectional area / fiber volume

Average cross-sectional areas varied across DIAm fiber types ($F_{(2.177)}= 59.1$, $p<0.0001$, one-way ANOVA; Figure 1B), with type I (604 ± 130 μm^2) and type IIa (678 ± 132 μm^2) fibers having a smaller cross-sectional area compared to type IIx/IIb fibers (3,070 ± 563 μm^2; $p<0.0001$ for both comparisons, Tukey's *post hoc* tests; Figure 1B). We observed no difference in cross-sectional area between type I and type IIa fibers ($p=0.47$, Tukey's *post hoc* tests; Figure 1B). Thus, the muscle fiber volumes of type IIx/IIb DIAm fibers were ~4.5–5.0 fold larger than those of type I and IIa fibers.

3.3 Mitochondrial volume across fiber types

Mitochondrial volume was measured in 15 fibers per type per DIAm from 6 animals (3 males, 3 females), and found to vary across fiber types ($F_{(2,267)}=1302.0$, $p<0.0001$, one-way ANOVA; Figure 4A). Mitochondrial volumes in type I (178 ± 41 μm^3) and type IIa (195 ± 34 μm^3) were lower than type IIx/IIb (622 ± 100 μm^3; $p<0.0001$ for both comparisons,

Tukey's *post hoc* tests; Figure 4A). There was no significant difference in mitochondrial volume between type I and type IIa fibers (p=0.22; Figure 4A).

3.4 Mitochondrial volume density across fiber types

Mitochondrial volume density was calculated in 15 fibers per type per DIAm from 6 animals (3 males, 3 females) by normalizing mitochondrial volume for muscle fiber volume (fiber cross-sectional area × 10 μm section thickness). Mitochondrial volume density varied across fiber types ($F_{(2,267)}$=176.9, p<0.0001, one-way ANOVA; Figure 4B), with type I (30 ± 6%) and type IIa (30 ± 5%) fibers having a greater mitochondrial volume density than type IIx/IIb fibers (16 ± 5%; p<0.0001 in both combinations, Tukey's *post hoc* tests; Figure 4B). There was no significant difference in mitochondrial volume density between type I and type IIa fibers (p=0.84, Tukey's *post hoc* test; Figure 4B).

3.5 Mitochondrial morphology across fiber types

Mitochondrial morphology (mean branch length and MCI) was measured in 15 fibers per type per DIAm from 6 animals (3 males, 3 females). Mean branch length varied across fiber type ($F_{(2,268)}$=292.0, p<0.0001, one-way ANOVA; Figure 4C), being greater in type I (17.6 ± 4.2) and type IIa fibers (18.6 ± 5.2) compared to type IIx/IIb (5.0 ± 2.9; p<0.0001 in both combinations, Tukey's *post hoc* tests; Figure 4C). There was no significant difference in mean mitochondrial branch length between type I and type IIa fibers (p=0.21, Tukey's *post hoc* test; Figure 4C). MCI varied across fiber type ($F_{(2,268)}$=197.1, p<0.0001, one-way ANOVA), with MCI in type I (26.3 ± 6.9) and type IIa fibers (27.8 ± 7.2) greater than that in type IIx/IIb fibers (11.3 ± 3.9; <0.0001 in both combinations, Tukey's *post hoc* tests; Figure 4D). The MCI was comparable between type I and IIa (p=0.20, Tukey's *post hoc* test; Figure 4D). taken together, the higher mean branch length and MCI, indicated that the mitochondrial morphologies of type I and IIa fibers were more filamentous, while the mitochondrial morphology of type IIx/IIb was more fragmented.

3.6 SDH_{max} per DIAm fiber volume

SDH_{max} (normalized per muscle fiber volume) was measured in 15 fibers per type per DIAm from 6 animals (3 males, 3 females), and SDH_{max} was found to be dependent on fiber type ($F_{(2,267)}$=348.5, p<0.0001, one-way ANOVA; Figures 5A). The SDH_{max} of type I and IIa fibers was significantly greater than that of type IIx/IIb fibers (p<0.0001 in both comparisons, Tukey's *post hoc* test; Figures 2B and 5A). There was no significant difference in SDH_{max} between type I and type IIa fibers (p=0.95, Tukey's *post hoc* test Figures 5A).

3.7 SDH_{max} per mitochondrial volume

SDH_{max} was also normalized for mitochondrial volume in 15 fibers per type per DIAm from 6 animals (3 males, 3 females) and found to vary across fiber types (Figure 5B). The SDH_{max} per mitochondrial volume was higher in type I and IIa DIAm fibers compared to type IIx/IIb fibers ($F_{(2,267)}$=407.4, p<0.0001, one-way ANOVA; p=0.01, Tukey's *post hoc* test; Figure 5B). Importantly, no difference in SDH_{max} per mitochondrial volume was found between type I and type IIa fibers (p>0.99, Tukey's *post hoc* test).

Within DIAm fibers, SDH_{max} was compared to different mitochondrial parameters including mitochondrial volume, volume density, mean branch length, and MCI. When comparing SDH_{max} per fiber volume to each of the mitochondrial parameters, two distinct clusters of DIAm fibers were apparent, type I and IIa fibers versus type IIx/IIb fibers. Type I and IIa DIAm fibers had higher SDH_{max} per fiber volume and higher mitochondrial volume densities as compared to type IIx/IIb fibers ($p<0.0001$, runs test; Figure 6A). Type I and IIa DIAm fibers had lower total mitochondrial volume than type IIx/IIb fibers, but the ~5-fold difference in fiber cross-sectional areas (Figure 1) resulted in significantly larger mitochondrial volume densities in type I and IIa fibers ($p<0.0001$, runs test) (Figure 6A). The higher SDH_{max} per mitochondrial volume in the type I and IIa DIAm fibers was associated with a higher MCI, indicative of more filamentous mitochondria, while mitochondrial in type IIx/IIb fibers were more fragmented (lower mean branch length and lower MCI ($p<0.0001$, runs test) (Figure 6B).

4. DISCUSSION

The major novel findings of the present study are: i) mitochondrial volume density is higher in type I and type IIa compared to type IIx/IIb fibers, ii) mitochondria in type I and IIa fibers are more filamentous than in type IIx/IIb fibers, iii) SDH_{max} reflects the maximum respiratory capacity of DIAm fibers and is higher in type I and type IIa fibers compared to type IIx/IIb fibers, iv) SDH_{max} per mitochondrial volume is higher in type I and IIa fibers than type IIx/IIb fibers, reflecting intrinsic differences in mitochondrial respiratory capacity across fiber types. Our novel results combining measures of mitochondrial function (SDH_{max}) and mitochondrial structure in the same fibers provide clear evidence that mitochondrial structure and function vary across different DIAm fiber types consistent with differences in their activation history.

4.1 Confocal imaging-based measurements of mitochondria in DIAm fibers

The present study utilized a confocal imaging-based technique for identifying and quantifying mitochondrial morphology in type identified DIAm fibers. MitoTracker Green, which was used to label mitochondria, accumulates in the mitochondrial matrix based on the proton gradient, where it covalently binds to mitochondrial thiol groups. MitoTracker Green labeling is dependent on an intact cell membrane and membrane potential. Thus, the mitochondria labeled using MitoTracker Green have to be functional, which depending on the research question may be either beneficial or a limitation.

In a previous study in rat DIAm fibers, we used 2-D EM to estimate mitochondrial volume densities in different fiber types (Sieck *et al.*, 1998). In this study, using 2-D EM, we found that type I and IIa DIAm fibers had mitochondrial volume densities of ~25%, whereas type IIx/IIb fibers had mitochondrial volume densities of ~3%. These results were qualitatively similar to differences in mitochondrial volume densities across fiber types reported by other groups (Mathieu *et al.*, 1981; Mathieu-Costello *et al.*, 2002; Gamboa & Andrade, 2010). In contrast, using 3-D confocal imaging of MitoTracker Green in the present study, we found the mitochondrial volume densities of type I and IIa DIAm fibers were comparable at ~30%, whereas the mitochondrial volume densities of type IIx/IIb fibers were higher at ~17%.

Measuring mitochondrial volume density using 2-D EM is very labor-intensive, which limits sample size. A major advantage of the confocal fluorescence microscopy technique is that many more fibers can be analyzed, and fiber type can be readily determined. In contrast, 2-D EM does not allow for direct assessment of fiber type. Since 2-D EM does not depend on an intact mitochondrial membrane and proton gradient, it does not distinguish between functional and non-functional mitochondria, which is another major advantage of the confocal technique based on MitoTracker Green labeling of mitochondria.

Mitochondrial morphology varied across fiber types. Mitochondria in type I and IIa DIAm fibers were more filamentous (increased mean branch length and MCI) than those in type IIx/IIb fibers. It has been reported that mitochondrial morphology can affect mitochondrial respiratory capacity (Peterson *et al.*, 2012; Ryan *et al.*, 2015; Ryan *et al.*, 2018; Vincent *et al.*, 2019; Delmotte *et al.*, 2021). For example, in a previous study, we found that maximum O_2 consumption rate of mitochondria in human airway smooth muscle (hASM) cells was higher when mitochondrial morphometry was more filamentous (Delmotte *et al.*, 2021). In another study, it was suggested that mitochondrial morphology is a distinguishing characteristic across muscle fiber types with type I and IIa being more filamentous and type IIx/IIb being more fragmented (Mishra *et al.*, 2015). Other studies found that filamentous morphology was the standard state in highly active tissues (Trewin *et al.*, 2018; Chaudhry *et al.*, 2020). Filamentous mitochondria have a higher surface area compared to volume (increased MCI), which suggests that there is also a higher inner mitochondrial membrane surface area, the structural substrate for O_2 consumption and oxidative phosphorylation. We propose that our observations of greater mitochondrial respiratory capacities (SDH_{max} per mitochondrial volume) of type I and IIa fibers in the DIAm are due to their incessant activity in supporting breathing.

4.2 SDH_{max} measurements in DIAm fibers

The method for measuring SDH_{max} was developed in our laboratory and first reported in 1986 (Sieck *et al.*, 1986), with greater detail provided in a subsequent publication (Blanco *et al.*, 1988). The quantitative histochemical technique uses 1-methoxyphenzaine methosulfate (mPMS) as an exogenous electron carrier and azide to inhibit cytochrome oxidase (Complex IV) and thereby reduce non-specific reduction of NBT in the reaction. As previously reported (Sieck *et al.*, 1986; Blanco & Sieck, 1987; Blanco *et al.*, 1988; Enad *et al.*, 1989; Sieck *et al.*, 1989; Watchko & Sieck, 1993; Proctor *et al.*, 1995; Sieck *et al.*, 1995; Sieck *et al.*, 1996; Zhan *et al.*, 1997), we confirmed that the SDH reaction is highly linear over a 10 min period, limited by substrate (succinate) availability and dependent on pathlength (tissue section thickness). The present study extends the validation of this quantitative histochemical technique by showing that SDH_{max} is insensitive to FCCP-mediated disruption of the mitochondrial proton gradient, and is inhibited by rotenone, a Complex I inhibitor and antimycin A, a Complex III inhibitor. The SDH_{max} technique has also been validated in other labs, notably, by Powers et. al (Powers *et al.*, 1993). Thus, there is converging evidence that this technique is rigorous and reproducible and that SDH_{max} provides an excellent surrogate for measurements of maximum mitochondrial respiration, similar to that obtained using respirometry. Using pharmacological techniques similar to those used in respirometry studies, SDH_{max} was identical to rates obtained using FCCP,

which decouples cellular respiration from the proton gradient and allows for determination of the maximum O_2 consumption rate (Gullans *et al.*, 1982; Sipos *et al.*, 2003). In the present study, we also showed that the SDH_{max} measurements within a single DIAm fiber varied by ~10–15% along the length of the entire fiber.

In the present study, both type I and IIa fibers in the rat DIAm had higher SDH_{max} than type IIx/IIb fibers. This is consistent with past reports in the rat DIAm (Sieck *et al.*, 1989; Johnson & Sieck, 1993; Sieck *et al.*, 1995; Lattari *et al.*, 1997; Zhan *et al.*, 1997; Fogarty *et al.*, 2020) as well as the cat DIAm (Sieck *et al.*, 1986; Enad *et al.*, 1989; Sieck *et al.*, 1991). There are also similar differences in SDH_{max} across fiber types in other skeletal muscles of the rat (Watchko & Sieck, 1993; Blanco *et al.*, 1995) and other species (Blanco *et al.*, 1991; Lewis *et al.*, 1992; Howell *et al.*, 1995; Sieck *et al.*, 1996) including humans (Proctor *et al.*, 1996). Although in all cases, the SDH_{max} of type I and IIa fibers was reported to be higher than that of type IIx/IIb fibers, there are differences in SDH_{max} within a fiber type. For example, the SDH_{max} of type I and IIa fibers in the DIAm is higher than that of type I and IIa fibers in the medial gastrocnemius muscle. The type IIx/IIb fibers were less consistent when comparing to DIAm.

The higher SDH_{max} of type I and type IIa DIAm fibers is consistent with their frequent activation (~40% duty cycle) in sustaining breathing and ensuring adequate ventilation (Sieck & Fournier, 1989; Sieck, 1991; Fogarty & Sieck, 2019). Similarly, the substantially lower SDH_{max} in type IIx/IIb DIAm fibers is consistent with their infrequent activation (<1% duty cycle) only during expulsive behaviors (Sieck & Fournier, 1989; Sieck, 1991; Fogarty & Sieck, 2019). Accordingly, energy requirements are likely to differ greatly across DIAm fiber types.

4.3 Concurrent measurements of mitochondrial volume density and SDH_{max} in DIAm fibers

In the present study, sequential sections measuring SDH_{max}, mitochondrial volume density, and MyHC fiber typing allows for measurements of all these properties within the same fiber. This nuanced evaluation of the DIAm in type-identified fibers allows us to relate mitochondrial function (SDH_{max}) with mitochondrial content (mitochondrial volume). In a previous study using Sprague-Dawley rats, we evaluated mitochondrial volume density using EM according to fiber types established by MyHC expression in serial sections (Sieck *et al.*, 1998). When comparing that prior study to the present study, we see a good agreement in type I and IIa fibers, with mitochondrial volume density of type I fibers being ~28% (Sieck *et al.*, 1998) and ~30%, respectively. Similarly, negligible differences were observed in type IIa fibers, with mean mitochondrial volumed densities being ~22 % for EM (Sieck *et al.*, 1998) compared to ~30% for fluorescence. By contrast more variability was observed in type IIx and/or IIb fibers, with mitochondrial volume density being ~3% in EM (Sieck *et al.*, 1998) estimates compared to ~16% for fluorescence. The difference between these measurements is likely due to sampling. In the EM data, eight fibers of each type were sampled across five rats. In the confocal fluorescent microscopy measurements, fifteen fibers of each type were sampled from six rats of both sexes. Regardless, the only significant changes are those observed between type I and IIa fibers compared to IIx and/or IIb fibers.

Measuring mitochondrial volume using fluorescent confocal microscopy provides distinct benefits compared to EM, and in our current study, it allows us to measure the mitochondrial volume within the same fibers that we measure SDH_{max}.

4.4 Maximum mitochondrial respiratory capacity (SDH_{max}) varies across fiber types

Our results confirmed that the SDH_{max} measurement reflected the maximum respiratory capacity of muscle fibers. SDH_{max} of different DIAm fiber types varied independently of mitochondrial volume. Type IIx/IIb DIAm fibers had higher total mitochondrial volumes than type I and IIa fibers, but their SDH_{max}. In contrast, because of their smaller cross-sectional areas, the mitochondrial volume densities of type I and IIa DIAm fibers were greater as compared to type IIx/IIb fibers. When directly comparing SDH_{max} to either mitochondrial volume or mitochondrial volume density no correlation existed, but two clusters of fibers were apparent. Type I and IIa fibers clustered with higher SDH_{max} and mitochondrial volume densities (or lower total mitochondrial volumes). When SDH_{max} was normalized to mitochondrial volume to reflect the maximum respiratory capacity per mitochondrial volume, type I and IIa DIAm fibers have much greater SDH_{max} per mitochondrial volume as compared to type IIx/IIb fibers. This implies that there are inherent differences between mitochondria in type I and IIa DIAm fibers vs type IIx/IIb fibers. One possibility relates to the differences in mitochondrial morphology across fiber types.

4.5 Conclusions

In conclusion, we found that SDH_{max} and mitochondrial volume density are higher in type I and IIa fibers in the rat DIAm compared to type IIx/IIb fibers. In addition, we found that mitochondria are more filamentous in type I and type IIa DIAm fibers than type IIx/IIb fibers. Importantly, SDH_{max} per mitochondrial volume was higher in type I and IIa DIAm fibers, which may relate to the increased duty cycle of these fibers in sustaining breathing.

Acknowledgements:

We would like to thank Rebecca Macken, Yun-Hua Fang, Dr. Philippe Delmotte, and Dr. Wen-Zhi Zhan for their assistance in this project.

Funding:

This work was supported by National Institutes of Health grants R01-AG044615 (GCS), R01-HL146114 (GCS) and T32-HL105355 (ADB).

REFERENCES

Aravamudan B, Kiel A, Freeman M, Delmotte P, Thompson M, Vassallo R, Sieck GC, Pabelick CM & Prakash YS. (2014). Cigarette smoke-induced mitochondrial fragmentation and dysfunction in human airway smooth muscle. Am J Physiol Lung Cell Mol Physiol 306, L840–854. [PubMed: 24610934]

Blanco CE, Fournier M & Sieck GC. (1991). Metabolic variability within individual fibres of the cat tibialis posterior and diaphragm muscles. Histochemical Journal 23, 366–374.

Blanco CE, Micevych PE, Zhan WZ & Sieck GC. (1995). Succinate dehydrogenase activity of sexually dimorphic muscles of rats. J Appl Physiol 78, 2147–2152. [PubMed: 7665411]

Blanco CE & Sieck GC. (1987). Comparison of succinate dehydrogenase activity between the diaphragm and medial gastrocnemius muscles of the rat. In Respiratory Muscles and Their

Neuromotor Control, ed. Sieck GC, Gandevia SC & Cameron WE, pp. 281–289. Alan R. Liss, Inc., New York.

Blanco CE, Sieck GC & Edgerton VR. (1988). Quantitative histochemical determination of succinic dehydrogenase activity in skeletal muscle fibres. Histochemical Journal 20, 230–243.

Chaudhry A, Shi R & Luciani DS. (2020). A pipeline for multidimensional confocal analysis of mitochondrial morphology, function, and dynamics in pancreatic β-cells. Am J Physiol Endocrinol Metab 318, E87–e101. [PubMed: 31846372]

Delmotte P, Marin Mathieu N & Sieck GC. (2021). TNFα induces mitochondrial fragmentation and biogenesis in human airway smooth muscle. Am J Physiol Lung Cell Mol Physiol 320, L137–l151. [PubMed: 33146568]

Delmotte P & Sieck GC. (2019). Endoplasmic Reticulum Stress and Mitochondrial Function in Airway Smooth Muscle. Front Cell Dev Biol 7, 374. [PubMed: 32010691]

Delmotte P, Zavaletta VA, Thompson MA, Prakash YS & Sieck GC. (2017). TNFalpha decreases mitochondrial movement in human airway smooth muscle. Am J Physiol Lung Cell Mol Physiol 313, L166–L176. [PubMed: 28473328]

Donoho DL & Johnstone IM. (1994). Ideal spatial adaptation by wavelet shrinkage. Biometrika 81, 425–455.

Enad JG, Fournier M & Sieck GC. (1989). Oxidative capacity and capillary density of diaphragm motor units. J Appl Physiol 67, 620–627. [PubMed: 2529236]

Fogarty MJ, Mantilla CB & Sieck GC. (2019). Impact of sarcopenia on diaphragm muscle fatigue. Exp Physiol 104, 1090–1099. [PubMed: 30924589]

Fogarty MJ, Marin Mathieu N, Mantilla CB & Sieck GC. (2020). Aging Reduces Succinate Dehydrogenase Activity in Rat Type IIx/IIb Diaphragm Muscle Fibers. J Appl Physiol (1985).

Fogarty MJ, Omar TS, Zhan WZ, Mantilla CB & Sieck GC. (2018). Phrenic Motor Neuron Loss in Aged Rats. J Neurophysiol 119, 1852–1862. [PubMed: 29412773]

Fogarty MJ, Rana S, Mantilla CB & Sieck GC. (2021). Quantifying mitochondrial volume density in phrenic motor neurons. J Neurosci Methods 353, 109093. [PubMed: 33549636]

Fogarty MJ & Sieck GC. (2019). Evolution and Functional Differentiation of the Diaphragm Muscle of Mammals. Compr Physiol 9, 715–766. [PubMed: 30873594]

Gamboa JL & Andrade FH. (2010). Mitochondrial content and distribution changes specific to mouse diaphragm after chronic normobaric hypoxia. Am J Physiol Regul Integr Comp Physiol 298, R575–583. [PubMed: 20007520]

Geiger PC, Bailey JP, Mantilla CB, Zhan WZ & Sieck GC. (2006). Mechanisms underlying myosin heavy chain expression during development of the rat diaphragm muscle. J Appl Physiol 101, 1546–1555. [PubMed: 16873604]

Geiger PC, Cody MJ, Macken RL & Sieck GC. (2000). Maximum specific force depends on myosin heavy chain content in rat diaphragm muscle fibers. J Appl Physiol 89, 695–703. [PubMed: 10926656]

Geiger PC, Cody MJ & Sieck GC. (1999). Force-calcium relationship depends on myosin heavy chain and troponin isoforms in rat diaphragm muscle fibers. J Appl Physiol 87, 1894–1900. [PubMed: 10562634]

Gullans SR, Brazy PC, Soltoff SP, Dennis VW & Mandel LJ. (1982). Metabolic inhibitors: effects on metabolism and transport in the proximal tubule. Am J Physiol 243, F133–140. [PubMed: 7114212]

Han YS, Geiger PC, Cody MJ, Macken RL & Sieck GC. (2003). ATP consumption rate per cross bridge depends on myosin heavy chain isoform. J Appl Physiol 94, 2188–2196. [PubMed: 12588786]

Howell S, Maarek JM, Fournier M, Sullivan K, Zhan WZ & Sieck GC. (1995). Congestive heart failure: differential adaptation of the diaphragm and latissimus dorsi. J Appl Physiol 79, 389–397. [PubMed: 7592193]

Jacques M, Kuang J, Bishop DJ, Yan X, Alvarez-Romero J, Munson F, Garnham A, Papadimitriou I, Voisin S & Eynon N. (2020). Mitochondrial respiration variability and simulations in human skeletal muscle: The Gene SMART study. Faseb j 34, 2978–2986. [PubMed: 31919888]

Johnson BD & Sieck GC. (1993). Activation-induced reduction of SDH activity in diaphragm muscle fibers. J Appl Physiol 75, 2689–2695. [PubMed: 8125891]

Koopman WJ, Verkaart S, Visch HJ, van der Westhuizen FH, Murphy MP, van den Heuvel LW, Smeitink JA & Willems PH. (2005a). Inhibition of complex I of the electron transport chain causes O2-. -mediated mitochondrial outgrowth. American journal of physiology Cell physiology 288, C1440–1450. [PubMed: 15647387]

Koopman WJ, Visch HJ, Smeitink JA & Willems PH. (2006). Simultaneous quantitative measurement and automated analysis of mitochondrial morphology, mass, potential, and motility in living human skin fibroblasts. Cytometry Part A : the journal of the International Society for Analytical Cytology 69, 1–12. [PubMed: 16342116]

Koopman WJ, Visch HJ, Verkaart S, van den Heuvel LW, Smeitink JA & Willems PH. (2005b). Mitochondrial network complexity and pathological decrease in complex I activity are tightly correlated in isolated human complex I deficiency. American journal of physiology Cell physiology 289, C881–890. [PubMed: 15901599]

Lattari A, Daood MJ, Sieck GC & Watchko JF. (1997). Rat diaphragm oxidative capacity, antioxidant enzymes, and fatigue: Newborn versus adult. Pediatr Res 42, 60–65. [PubMed: 9212038]

Lewis MI, Monn SA & Sieck GC. (1992). Effect of corticosteroids on diaphragm fatigue, SDH activity, and muscle fiber size. J Appl Physiol 72, 293–301. [PubMed: 1537729]

Ly CH & Ryall JG. (2017). Measuring Mitochondrial Substrate Utilization in Skeletal Muscle Stem Cells. Methods Mol Biol 1668, 61–73. [PubMed: 28842902]

Mathieu-Costello O, Morales S, Savolainen J & Vornanen M. (2002). Fiber capillarization relative to mitochondrial volume in diaphragm of shrew. J Appl Physiol (1985) 93, 346–353. [PubMed: 12070224]

Mathieu O, Krauer R, Hoppeler H, Gehr P, Lindstedt SL, Alexander RM, Taylor CR & Weibel ER. (1981). Design of the mammalian respiratory system. VII. Scaling mitochondrial volume in skeletal muscle to body mass. Respir Physiol Neurobiol 44, 113–128.

Mishra P, Varuzhanyan G, Pham AH & Chan DC. (2015). Mitochondrial Dynamics is a Distinguishing Feature of Skeletal Muscle Fiber Types and Regulates Organellar Compartmentalization. Cell Metab 22, 1033–1044. [PubMed: 26603188]

Peterson CM, Johannsen DL & Ravussin E. (2012). Skeletal Muscle Mitochondria and Aging: A Review. Journal of Aging Research 2012, 194821. [PubMed: 22888430]

Powers SK, Lieu F-K, Criswell D & Dodd S. (1993). Biochemical verification of quantitative histochemical analysis of succinate dehydrogenase activity in skeletal muscle fibres. The Histochemical Journal 25, 491–496. [PubMed: 8407360]

Prakash YS, Fournier M & Sieck GC. (1993a). Effects of prenatal undernutrition on developing rat diaphragm. J Appl Physiol 75, 1044–1052. [PubMed: 8226510]

Prakash YS, Smithson KG & Sieck GC. (1993b). Measurements of motoneuron somal volumes using laser confocal microscopy: comparisons with shape-based stereological estimations. Neuroimage 1, 95–107. [PubMed: 9343561]

Prakash YS, Smithson KG & Sieck GC. (1994). Application of the Cavalieri principle in volume estimation using laser confocal microscopy. Neuroimage 1, 325–333. [PubMed: 9343582]

Proctor DN, Joyner MJ & Sieck GC. (1996). Correlation between myosin heavy chain expression and actomyosin ATPase activity in human muscle fibers. FASEB J (Abstract) 10, A129.

Proctor DN, Sinning WE, Walro JM, Sieck GC & Lemon PWR. (1995). Oxidative capacity of human muscle fiber types: Effects of age and training status. J Appl Physiol 78, 2033–2038. [PubMed: 7665396]

Ryan ZC, Craig TA, Folmes CD, Wang X, Lanza IR, Schaible NS, Salisbury JL, Nair KS, Terzic A, Sieck GC & Kumar R. (2015). 1α,25-Dihydroxyvitamin D 3 Regulates Mitochondrial Oxygen Consumption and Dynamics in Human Skeletal Muscle Cells. Journal of Biological Chemistry.

Ryan ZC, Craig TA, Folmes CD, Wang X, Lanza IR, Schaible NS, Salisbury JL, Nair KS, Terzic A, Sieck GC & Kumar R. (2016). 1alpha,25-Dihydroxyvitamin D3 Regulates Mitochondrial Oxygen Consumption and Dynamics in Human Skeletal Muscle Cells. J Biol Chem 291, 1514–1528. [PubMed: 26601949]

Ryan ZC, Craig TA, Wang X, Delmotte P, Salisbury JL, Lanza IR, Sieck GC & Kumar R. (2018). 1alpha,25-dihydroxyvitamin D3 mitigates cancer cell mediated mitochondrial dysfunction in human skeletal muscle cells. Biochemistry and Biophysic Research Communications 496, 746–752.

Sieck GC. (1991). Neural control of the inspiratory pump. NIPS 6, 260–264.

Sieck GC, Cheung TS & Blanco CE. (1991). Diaphragm capillarity and oxidative capacity during postnatal development. J Appl Physiol 70, 103–111. [PubMed: 1826289]

Sieck GC & Fournier M. (1989). Diaphragm motor unit recruitment during ventilatory and nonventilatory behaviors. J Appl Physiol 66, 2539–2545. [PubMed: 2745316]

Sieck GC, Fournier M, Prakash YS & Blanco CE. (1996). Myosin phenotype and SDH enzyme variability among motor unit fibers. J Appl Physiol 80, 2179–2189. [PubMed: 8806928]

Sieck GC, Han YS, Prakash YS & Jones KA. (1998). Cross-bridge cycling kinetics, actomyosin ATPase activity and myosin heavy chain isoforms in skeletal and smooth respiratory muscles. Comp Biochem Physiol 119, 435–450.

Sieck GC, Lewis MI & Blanco CE. (1989). Effects of undernutrition on diaphragm fiber size, SDH activity, and fatigue resistance. J Appl Physiol 66, 2196–2205. [PubMed: 2745285]

Sieck GC, Mantilla CB & Prakash YS. (1999). Volume measurements in confocal microscopy. Methods Enzymol 307, 296–315. [PubMed: 10506980]

Sieck GC, Sacks RD, Blanco CE & Edgerton VR. (1986). SDH activity and cross-sectional area of muscle fibers in cat diaphragm. J Appl Physiol 60, 1284–1292. [PubMed: 2939051]

Sieck GC, Zhan WZ, Prakash YS, Daood MJ & Watchko JF. (1995). SDH and actomyosin ATPase activities of different fiber types in rat diaphragm muscle. J Appl Physiol 79, 1629–1639. [PubMed: 8594023]

Sipos I, Tretter L & Adam-Vizi V. (2003). Quantitative relationship between inhibition of respiratory complexes and formation of reactive oxygen species in isolated nerve terminals. J Neurochem 84, 112–118. [PubMed: 12485407]

Trewin AJ, Berry BJ & Wojtovich AP. (2018). Exercise and Mitochondrial Dynamics: Keeping in Shape with ROS and AMPK. Antioxidants (Basel) 7.

Vincent AE, White K, Davey T, Philips J, Ogden RT, Lawless C, Warren C, Hall MG, Ng YS, Falkous G, Holden T, Deehan D, Taylor RW, Turnbull DM & Picard M. (2019). Quantitative 3D Mapping of the Human Skeletal Muscle Mitochondrial Network. Cell Rep 26, 996–1009.e1004. [PubMed: 30655224]

Watchko JF & Sieck GC. (1993). Respiratory muscle fatigue resistance relates to myosin phenotype and SDH activity during development. J Appl Physiol 75, 1341–1347. [PubMed: 8226549]

Zhan WZ, Miyata H, Prakash YS & Sieck GC. (1997). Metabolic and phenotypic adaptations of diaphragm muscle fibers with inactivation. J Appl Physiol 82, 1145–1153. [PubMed: 9104851]

Highlights:

- Mitochondrial volume density is higher in type I and IIa than type IIx/IIb fibers
- Mitochondria in type I and IIa fibers are more filamentous than type IIx/IIb fibers
- SDH_{max} per unitary mitochondrial volume is higher in type I and IIa than type IIx/IIb fibers

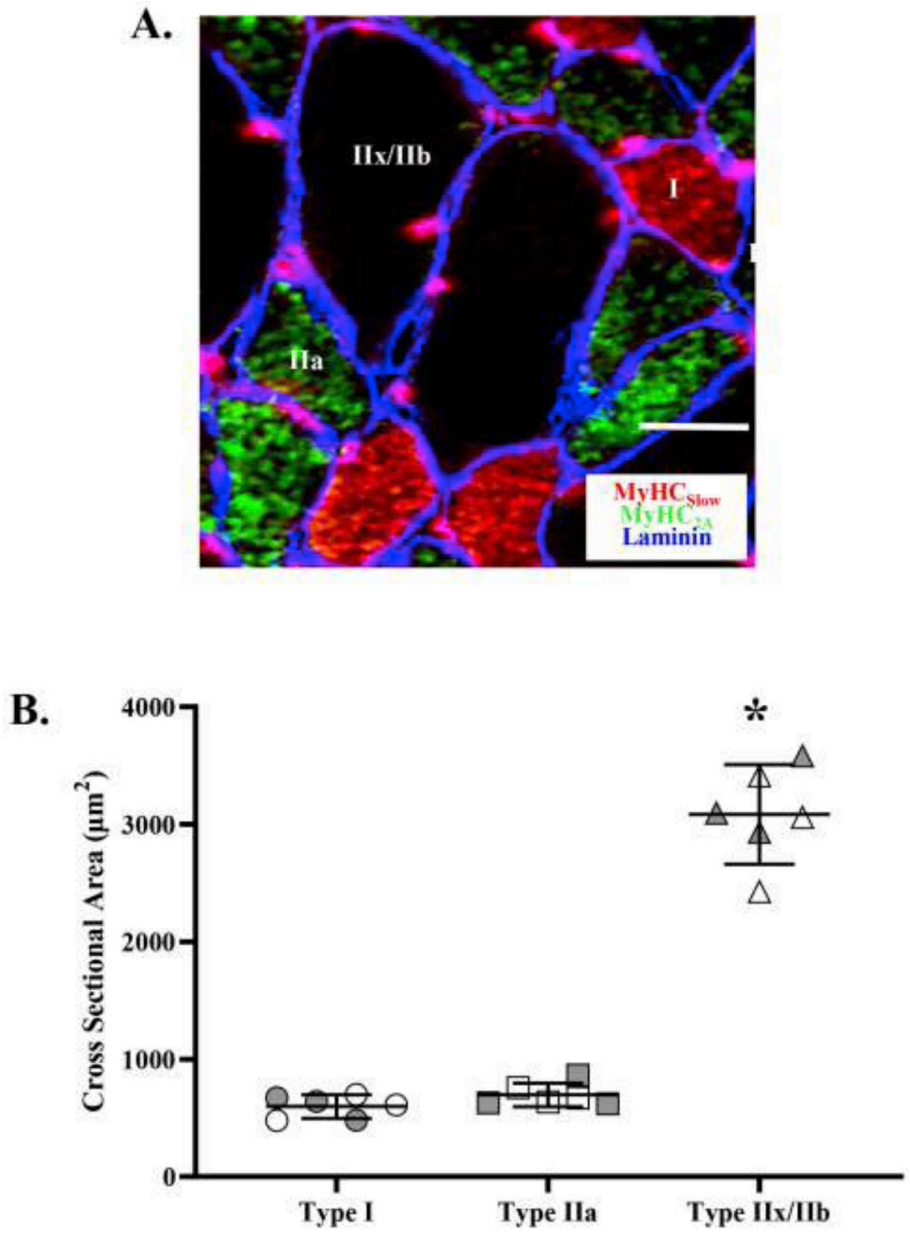

Figure 1:

A. DIAm fibers were classified based on immunoreactivity to anti-$MyHC_{Slow}$, anti-$MyHC_{2A}$, anti-$MyHC_{2X}$, and anti-$MyHC_{All\text{-}but\text{-}2X}$. The photomicrograph shows representative immunoreactivity to anti-$MyHC_{Slow}$ and anti-$MyHC_{2A}$ in the same DIAm section using an IgG-Alexa-594 (red) and IgM-Cy5 (green) secondary antibody, respectively. Type IIx/IIb fibers were classified based on immunoreactivity to anti-$MyHC_{2X}$ and no or partial immunoreactivity to anti-$MyHC_{All\text{-}but\text{-}2X}$. Laminin immunoreactivity (blue) was used to help define muscle fiber sarcolemma. **B.** Cross-sectional areas varied across DIAm fiber types ($p<0.001$; one-way ANOVA). The cross-sectional areas of type I and IIa DIAm fibers were comparable and signficantly small than those of type IIx/IIb fibers ($p<0.001$; Tukey's *post hoc* test). For each comparison n=15 fibers per type per animal (6

animals – 3 females and 3 males) with females indicated by grey shading. * denotes $p<0.05$. Scale Bar = 10 μm.

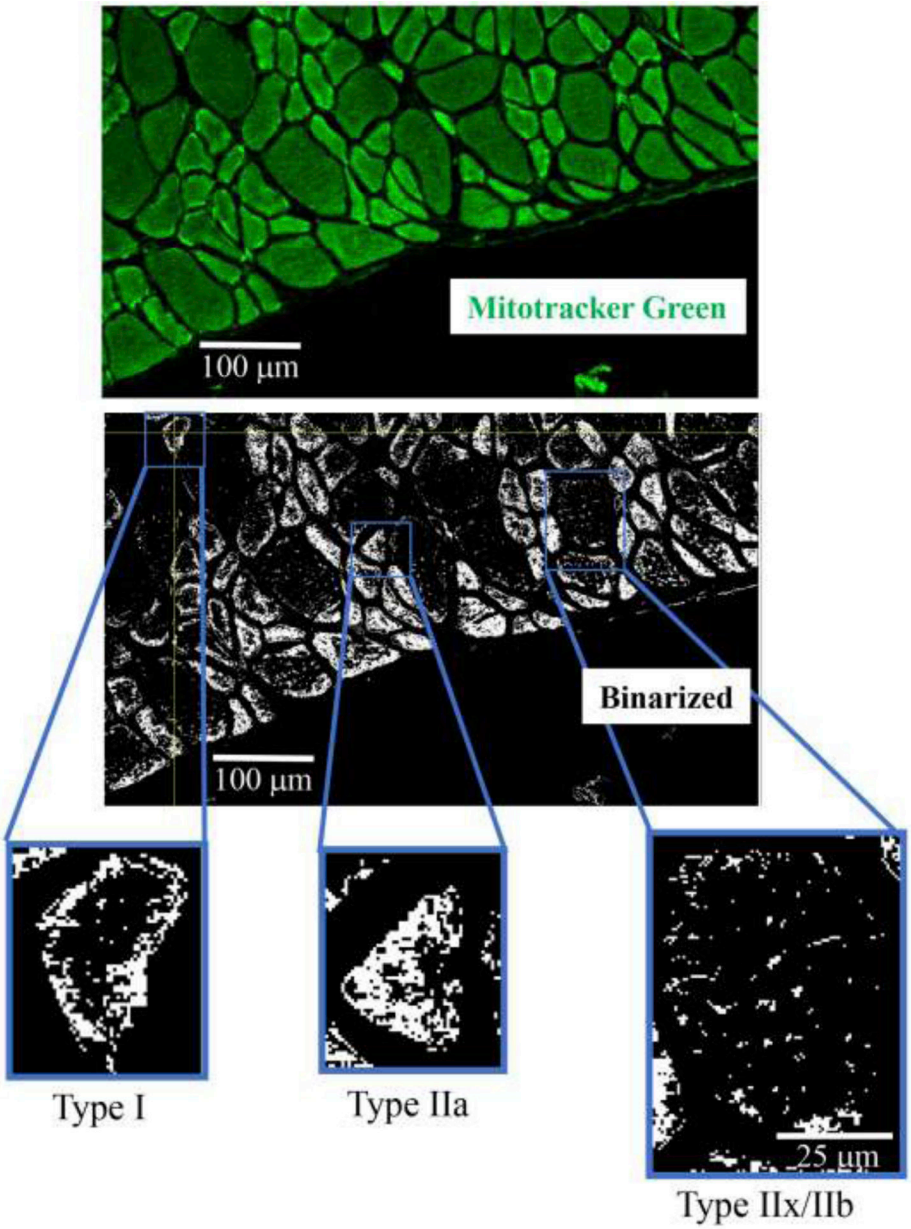

Figure 2:

Mitochondria in DIAm fibers were labeled using MitoTracker Green (upper photomicrograph) in alternate serial sections (same fibers used for fiber type classification and SDH_{max} measurements) cut at 10 µm thickness. MitoTracker Green fluorescence was visualized using Olympus FV2000 laser scanning confocal microscope and fluorescence intensity thresholded to create binary images of labeled mitochondria (middle photomicrograph). Representative binarized images of mitochondria in type I, IIa and IIx/IIb DIAm fibers are shown in the lower photomicrographs.

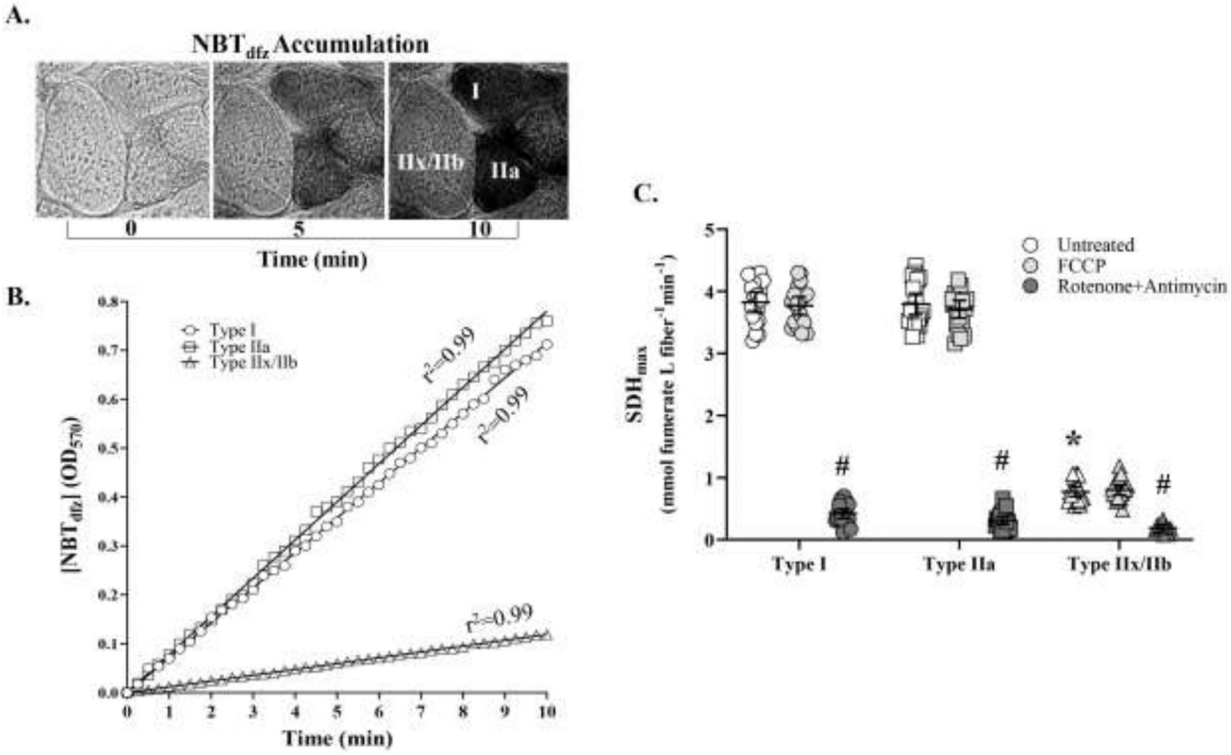

Figure 3:

In the SDH reaction, the acccumulation of [NBT_{dfz}] in muscle fibers was measured every 15 s across a 10 min period as the change in OD at 570 nm. **A.** Pictomicrographs show a representative example of the change in OD in type I, IIa and IIx/IIb DIAm fibers at 0, 5, and 10 min during the SDH reaction. **B.** In each DIAm fiber, the SDH reaction was linear (across the 10-min period (r^2>0.99) and the maximum veolicty of the SDH reaction (SDH_{max}) was calculated using the Beer-Lamber-Bouger law: $d[NBT_{dfz}]([fumarate]) = \frac{dOD}{kl}$. Where the average OD within a DIAm fiber measured every 15 s is divided by the molar extinction coefficient of NBT_{dfz} (*k;* 26,478 mol/cm) times the path length of light absorbance (*l;* 6 μm in this study). **C.** In type identified DIAm fibers, the SDH reaction (change in OD with time) was measured after addition of 1 mM carbonyl cyanide-p-trifluoromethoxyphenylhydrazone (FCCP), which disrupts the proton gradient uncoupling O_2 consumption from the electron transport chain (ETC). Note that FCCP had no effect on SDH_{max} in any fiber type. Treatment with 1 mM rotenone to inibit complex I of the ETC and 1 mM antimycin A inhibit complex III of the ETC markedly inhibited the SDH reaction in all DIAm fiber types (p<0.0001; Bonferroni *post hoc* test) providing a measure of basal [NBT_{dfz}] accumulation. In respirometry, changes in O_2 consumption rate after addition of FCCP, rotenone and antimycin A provide a measure of maximum mitochondrial respiratory capcity. The SDH_{max} (in untreated and after FCCP treatment) varied across DIAm fiber types (p<0.0001; two-way ANOVA). The SDH_{max} of type I and IIa DIAm fibers were comparable but both were significantly higher than the SDH_{max} of type IIx/IIb fibers (p<0.0001; Bonferroni *post hoc* test). For each comparison n=15 fibers per type per animal (6 animals – 3 females and 3 males). * denotes p< 0.05.

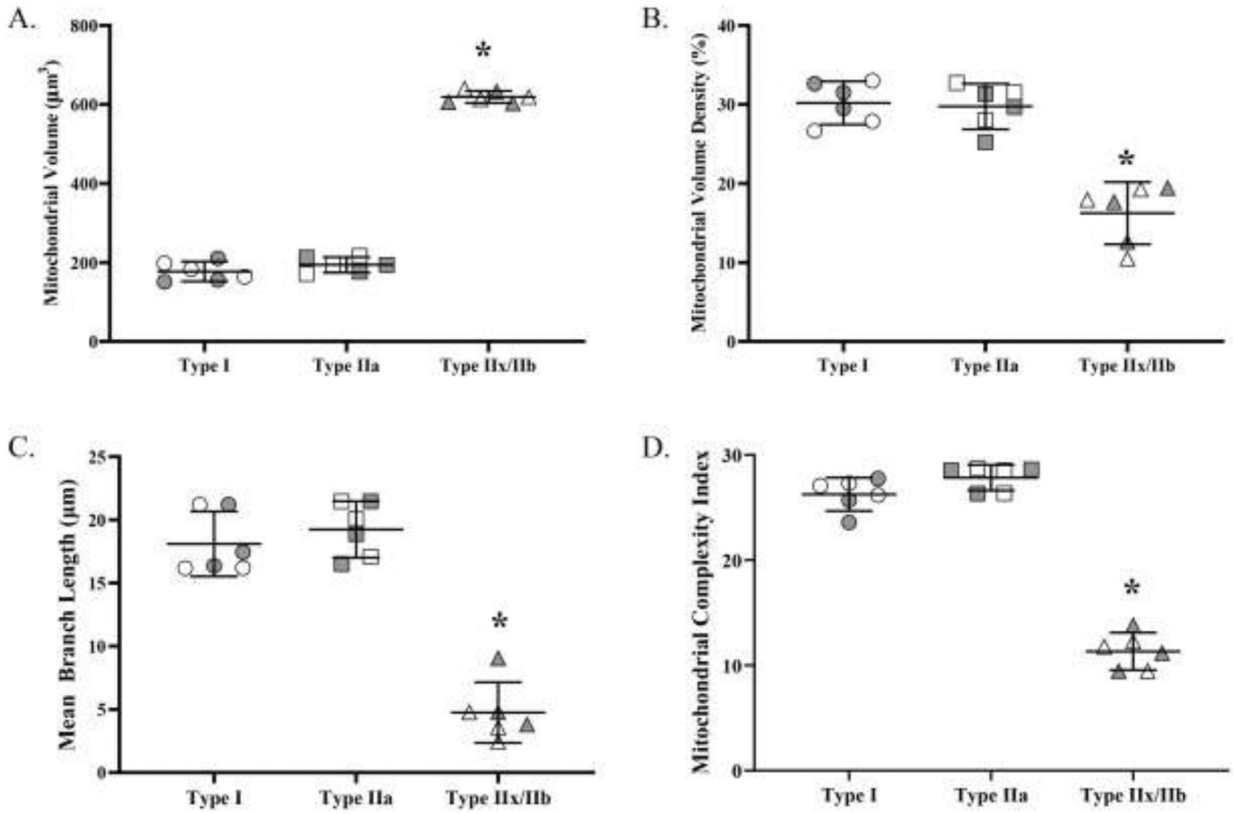

Figure 4:

A. Mitochondrial volume varied across DIAm fiber types (p<0.0001; one-way ANOVA). The mitochondrial volumes of type IIx/IIb fibers were significantly larger than those of both type I and IIa fibers (p<0.0001; Tukey's *post hoc* test) Mitochondrial volumes of type I and IIa fibers were not different. **B.** Mitochondrial volume density varied across fiber types (p<0.0001; one-way ANOVA). Mitochondrial volume densities in type I and type IIa DIAm fibers were comparable and significantly higher than mitochondrial volume density in type IIx/IIb fibers (p<0.0001; Tukey's *post hoc* test). **C.** The mean branch length varied across DIAm fiber types (p<0.001; one-way ANOVA). The mean branch lengths of type I and IIa were comparable but significantly longer than those of type IIx/IIb fibers (p<0.0001; Tukey's *post hoc* test). **D.** The MCI varied across DIAm fiber types (p<0.001; one-way ANOVA). The MCIs of type I and IIa were comparable but significantly larger than those of type IIx/IIb fibers (p<0.0001; Tukey's *post hoc* test). For each comparison n=15 fibers per type per animal (6 animals – 3 females and 3 males) with females indicated by grey shading. * denotes $p < 0.05$.

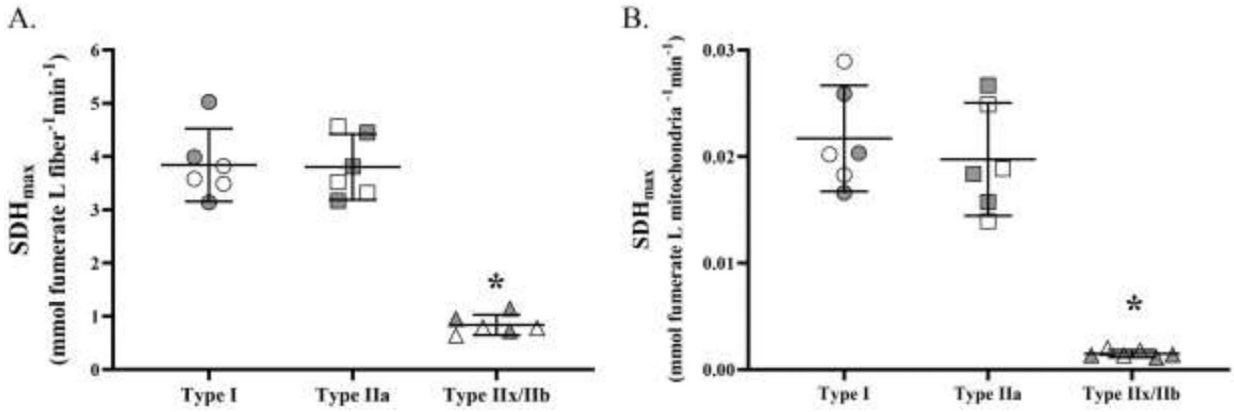

Figure 5:

A. SDH_{max} (per fiber volume) varied across fiber types ($p<0.0001$; one-way ANOVA). The SDH_{max} of type I and type IIa DIAm fibers were comparable but significantly higher than that in type IIx/IIb fibers ($p<0.0001$; Tukey's *post hoc* test). **B.** SDH_{max} was normalized for mitochondrial volume in each DIAm fiber. SDH_{max} per mitochondrial volume varied across fiber types ($p<0.0001$; one-way ANOVA). The SDH_{max} per mitochondrial volume of type I and IIa fibers were comparable but significantly higher than that of type IIx/IIb ($p<0.0001$; Tukey's *post hoc* test). For each comparison n=15 fibers per type per animal (6 animals – 3 females and 3 males) with females indicated by grey shading. * denotes $p< 0.05$.

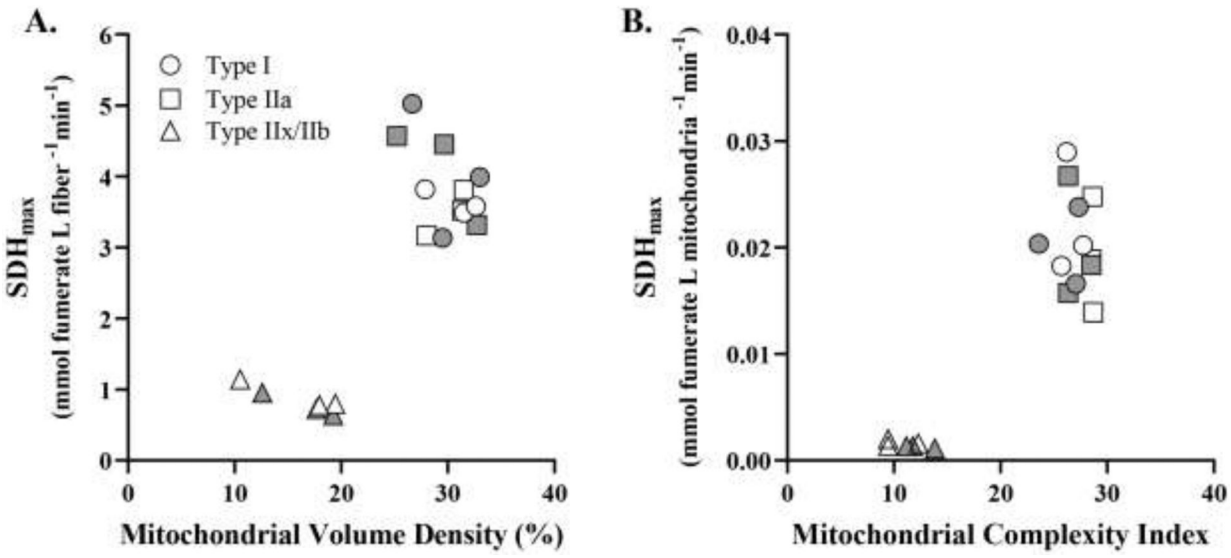

Figure 6:

A. Across DIAm fibers, the relationship between SDH_{max} per fiber volume and mitochondrial volume density identified two distinct clusters of fibers. In one group (type I and type IIa fibers), SDH_{max} per fiber volume and mitochondrial volume densities were higher, whereas in the second distinct group of type IIx/IIb fibers, SDH_{max} per fiber volume and mitochondrial volume densities were lower ($p<0.0001$, runs test). **B.** Across DIAm fibers, the relationship between SDH_{max} per mitochondrial volume and MCI also identified two distinct clusters of fibers. In the type I and type IIa DIAm fibers, SDH_{max} per mitochondrial volume and MCI were higher compared to values for type IIx/IIb fibers ($p<0.0001$, runs test). For each comparison n=15 fibers per type per animal (6 animals – 3 females and 3 males) with females indicated by grey shading.